Inorganic Chemistry
Article

Inorg. Chem. **2010**, *49*, 6853–6858 **6853**
DOI: 10.1021/ic1000733

Investigation of Ga Substitution in ZnO Powder and Opto-Electronic Properties

Hélène Serier, Alain Demourgues, and Manuel Gaudon*

CNRS, Université de Bordeaux 1, ICMCB, 87 avenue du Dr. Albert Schweitzer, 33608 Pessac, France

Received January 13, 2010

Two sets of Ga-doped ZnO powders were synthesized via solid-state and Pechini routes with a substitution rate varying from 0 to 4 mol %. The gallium solubility limit is strongly dependent on the synthesis history. Indeed, a low temperature annealing allows incorporating about 1.5 mol % (X-ray diffraction (XRD), inductive coupled plasma spectroscopy (ICP), optical properties) whereas under 0.1% of dopant is introduced after thermal treatment at high temperature: 1500 °C (from XRD and pellets conductivity). The incorporation of gallium leads to an anisotropic distortion of the zincite crystal lattice (*a* and *c* parameters increase and decrease, respectively, versus the Ga content leading to a decrease of the *c/a* ratio) which can be explained from the valence bond model. XRD analysis, chemical titration by ICP, and conductivity measurements (on pellets obtained at high temperature) allow determining accurately the maximum Ga content in the zincite. The optical properties (IR absorption efficiency) linked to electron carriers are directly correlated to the gallium rate introduced in ZnO oxide; nevertheless, the non linear correlation between these two parameters tends to show that the concentration of charge carriers in the system is not equal to the amount of Ga^{3+} atoms inserted per ZnO volume unit. A saturation regime is observed and was here explained once again on the basis of the valence band model by the increase of inhibiting p type defects with the increase of (n-type donors) Ga^{3+} concentration.

I. Introduction

Ga-doped ZnO compounds can be used as Al-doped ZnO powder (most developed) as transparent conductive oxides (TCOs), which are useful as transparent electrodes (opto-electronic devices),[1−12] or as thermal insulator films in smart windows (low emissive windows).[1−3] Indeed, ZnO is a large gap semiconductor with native n-type defects which accepts efficient doping by n-type donors as M^{3+} metallic elements or halogens as F^-. Even if gallium can be used as dopant (in very small quantity), maybe because of its expensive price and its storage in comparison with the large use of the Al^{3+} substitution, only few fundamental studies have been performed on Ga-doped ZnO. Nevertheless, gallium is a promising dopant for ZnO systems because of its ionic size and since the solubility limit of aluminum in zincite matrix is so low that the efficiency of the Ga-ZnO systems should be largely improved in comparison with the Al-ZnO ones.

In this study, it will be shown in a first part that the Ga^{3+} solubility limit can be tuned by the post-annealed treatment temperature applied to the oxide powder previously obtained by a soft chemistry synthesis process.

In a second step, the charge carrier concentration of the prepared Ga-doped ZnO powder was indirectly deduced from visible spectra.[13,14] Indeed, optical properties, and especially absorption in the near IR range, are linked to the ω_p plasma frequency, comparable to a "cut-off frequency" with regard to the electronic transport properties and therefore refractive index of the material: (i) if the incident wave is very energetic, that is, with a frequency higher than ω_p, the wave goes through the material without any interaction and no absorption; (ii) opposite to this, when the incident wave is less energetic, with a frequency lower than plasma one, the radiation is partially absorbed. Furthermore, the plasma frequency is directly related to the carrier concentration. Previously in our team[13] it was shown that the diffuse reflection, which is also the signature of the absorption, could be used to characterize free carriers. The variation of the charge

*To whom correspondence should be addressed. E-mail: gaudon@icmcb-bordeaux.cnrs.fr.

(1) Rubin, M. *Energy Res.* **1982**, *6*, 123–133.
(2) Hamberg, I.; Granqvist, C. G. *Sol. Energy Mater.* **1984**, *11*, 239–248.
(3) Lampert, C. M. *Sol. Energy Mater.* **1981**, *6*, 1–41.
(4) Rafla-Yuan, H.; Cordaro, J.F. *J. Appl. Phys.* **1991**, *69*, 959–964.
(5) Norman, V. J. *Aust. J. Chem.* **1969**, *22*, 325–329.
(6) Nie, D.; Xue, T.; Zhang, Y.; Li, X. *Sci. Chin., Series B: Chem.* **2008**, *51*, 823–828.
(7) Tsubota, T.; Ohataki, M.; Eguchi, K.; Arai, H. *J. Mater. Chem.* **1997**, *7*(1), 85–90.
(8) Strachowski, T.; Grzanka, E.; Lojkowski, W.; Presz, A.; Godlewski, M.; Yatsumento, S.; Matysiak, H.; Piticescu, R. R.; Monty, C. J. *J. Appl. Phys.* **2007**, *102*, 073513/1–073513/9.
(9) Roberts, N.; Wang, R.-P.; Sleight, A. W.; Warren, W. *Phys. Rev. B: Condens. Matter Mater. Phys.* **1998**, *57*, 4734–5741.
(10) Sugiyama, M.; Murayama, A.; Imao, T.; Saiki, K.; Nakanishi, H.; Chichibu, S. F. *Phys. Status Solidi* **2006**, *203*, 2882–2886.
(11) Wang, R.; Śleight, A. W.; Cleary, D. *Chem. Mater.* **1996**, *8*, 433–439.
(12) de Souza Goncalves, A.; Marques de Lima, S. A.; Davalos, M. R.; Antonio, S. G.; Paiva-Santos, C. *J. Sol-Gel Sci. Technol.* **2004**, *31*, 283–286.
(13) Serier, H.; Gaudon, M.; Ménétrier, M. *Solid State Sci.* **2009**, *11*(7), 1192–1197.
(14) Serier, H.; Gaudon, M.; Demourgues, A.; Tressaud, A. *J. Solid State Chem.* **2007**, *180*(12), 3485–349.

Published on Web 07/01/2010

carrier concentration versus the Ga^{3+} dopant concentration was finally interpreted. A model taking into account the occurrence of p-type defects supported by the Ga^{3+} ions introduction in the ZnO matrix was proposed.

II. Experimental Part

A first set of Ga-doped ZnO powder was prepared by a conventional solid state route; pellets of ZnO/Ga_2O_3 oxide mixture were pressed and sintered at 1500 °C under air for 10 h. A second set of powder was prepared via a polyesterification reaction based on the Pechini process.[15] This process allows the preparation of "low temperature" powder with a high specific area. This synthesis process is based on the chelation of metal ions by an α-hydroxyl acid such as citric acid to form stable homogeneous solutions. When mixed with a polyalcohol such as ethylene glycol, these solutions enable the polyesterification and the formation of a viscous brown resin by heating on a hot plate and removing excess solvent. The synthesis was performed with metal nitrates, citric acid, and ethylene glycol as starting materials, Pechini solution obeying the molar ratio 1:4:4 for metal salt/citric acid/ethylene glycol relative amounts. A first annealing at low temperature (400 °C for 5 h) removed the main part of the organic precursors; then, the intermediate black powder was ground in an agate mortar and heated up to 850 °C for 10 h under air. Powder compositions with 1−4 mol % of Ga^{3+} dopant were synthesized by this process. Additional calcinations under argon atmosphere at 700 °C for 10 h were also performed to create more charge carrier (n-type defects) in the zincite structure.

X-ray diffraction (XRD) patterns were collected using a PANalytical X'Pert MPD PW 3040 with Cu $K\alpha_1$ radiation (λ_1 = 1.540562 Å), and the measurements were performed with a scan step of 0.02° in the 2θ range from 5 to 130°. The FULLPROF program[16] was used for the pattern matching process and structural refinement.

The pellets' conductivity was determined by means of a four probe apparatus. The system consists in injecting a current intensity between the two exterior Pt probes and in measuring the generated potential difference between the two interior ones. This technique leads directly to the conductance; the Laplume shape factor K of the four probe apparatus has to be used to calculate the conductivity.[17]

UV−vis−NIR absorption properties were investigated by diffuse reflectance spectroscopy using a Cary 5000E spectrophotometer equipped with an integrating sphere in the wavelength region between 200 and 2500 nm. Samples were placed in a Suprasil cell equipped with a quartz window; halon standard (6 mm deep and 1 g/cm^3 density) was used as a white reference.

III. Results and Discussion

First, the influence of the synthesis temperature (850 or 1500 °C) and the atmosphere of synthesis (argon or air atmosphere) for the Pechini powder set was investigated on pure ZnO composition by high resolution XRD refinements. Neither the *a* and *c* cell parameters nor the z(O) free coordinate oxygen position are significantly affected by the synthesis parameters: the *a* parameter is equal to 3.2500(±1) Å in all cases; the *c* parameters is equal to 5.2053 Å, 5.2052 Å, and 5.2047 Å for 850 °C under air, 850 °C under argon, and 1500 °C under air, respectively; the z(O) coordinate is 0.383, 0.382, and 0.380 for 850 °C under air, 850 °C under argon, and 1500 °C under air, respectively. Hence it can be concluded that synthesis temperature and atmosphere have a marginal influence on the microstructural parameters.

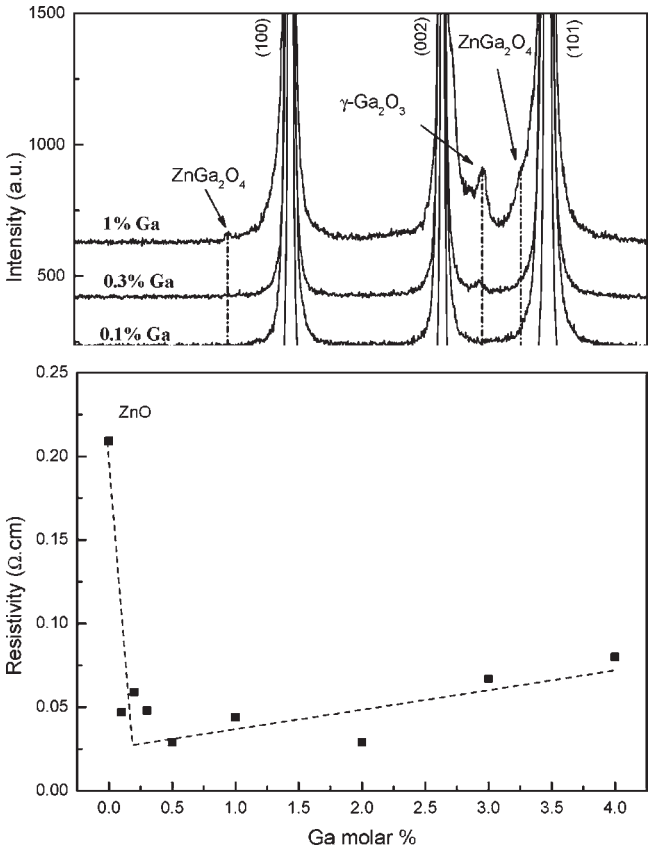

Figure 1. Powder XRD and pellet conductivity for various samples of $Zn_{1-x}Ga_xO$ target composition obtained the ceramic process.

Various Ga-doped ZnO pellets obtained after a high sintering treatment at 1500 °C under air were then analyzed by XRD. The corresponding patterns (a short 2θ window from 28 to 38° was chosen for more clarity) are reported in Figure 1-top. These analyses reveal the presence of an additional phase from 0.3 mol % of gallium: γ-Ga_2O_3 and $ZnGa_2O_4$ structure-type phases are both detected. The "thermodynamic" Ga^{3+} solubility limit (considering 1500 °C is a temperature for which the surface effect on the stabilization of gallium inside ZnO is negligible) is thus very low. The consequence of such a low solubility limit is the difficulty to evaluate accurately this solubility limit from XRD refinements. Indeed, the variation of cell parameters and atomic position versus the target gallium concentration is here found negligible, that is, about the same order as the error bar on these parameters (10^{-4} Å). Resistivity measurements are consequently here performed as indirect ways of determination of the gallium rate efficiently introduced.

The resistivity obtained on the corresponding various pellets is reported on the Figure 1-bottom. This resistivity decreases abruptly versus $x(Ga^{3+})$ from 0.2 Ω.cm (pure ZnO oxide) to 0.05 Ω.cm for all the doped samples. The observation of the same conductivity for a gallium concentration equal to 0.1 mol % or 2 mol % shows unambiguously that the solubility limit is below 0.1%. Nevertheless, the comparison between the undoped pellet and the other ones also shows unambiguously that all doped samples contain a part of the

(15) Pechini, M. P. U.S. Patent 3 330 697, 1967
(16) Rodriguez-Carvajal, J. Abstracts of the Satellite Meeting on Powder Diffraction of the XV Congress of the IUCr, 1990.
(17) Laplume, J. *L'onde électrique* **1955**, *335*, 113.

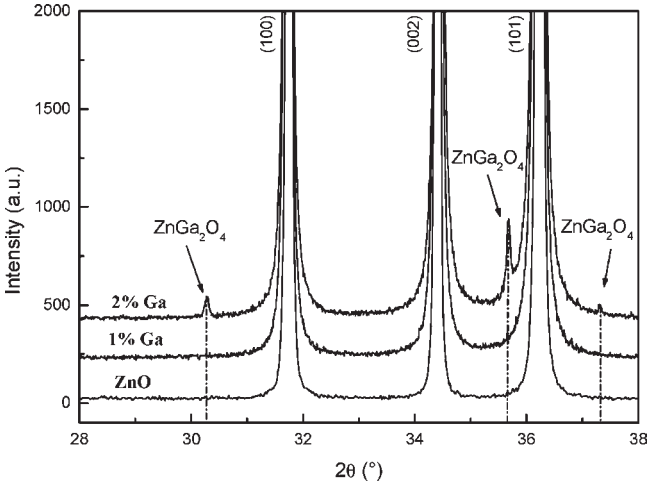

Figure 2. Powder XRD for various samples of $Zn_{1-x}Ga_xO$ target composition powder obtained by the Pechini process.

gallium in substitution or insertion in the zincite bulk structure. The slight linear increase of the resistivity versus the target gallium concentration from 0.1 through 4 mol % can be explained by the high resistivity of the observed impurities: Ga rich-phases forming over the solubility limit of Ga^{3+} in ZnO. Even if the γ-Ga_2O_3 and $ZnGa_2O_4$ structure-type phases are in very small proportion, one can suppose that they are segregated at the grain boundaries of the ZnO pellets leading to a measurable conductivity decrease.

Second, same Ga-doped ZnO compositions were synthesized at lower temperature from the Pechini process. Powder is obtained after calcinations at 850 °C under air. The same previous analyses by XRD were performed. The corresponding patterns are reported on the Figure 2. No secondary phase is detected for 1 mol % of gallium. The $ZnGa_2O_4$ secondary phase is detected only for the 2 mol % of Ga^{3+}. Hence, it can already be concluded that the Pechini process leads to a higher solubility limit of gallium inside ZnO than the solid state route. A profile matching was performed on the patterns of these powdered samples leading hence to the determination of *a* and *c* cell parameters. As shown in the Figure 3, the two parameters vary for low Ga content (below 2 mol %) and then remain quite stable for higher concentration. This confirms that Ga^{3+} solubility for the Pechini process in ZnO is about 1−2 mol %. This higher solubility limit in ZnO in comparison with the solid state process comes from surface effects. Indeed, after the 850 °C thermal treatment the Ga-doped ZnO grain size is still submicrometric whereas after sintering at 1500 °C the grains grow over micrometer. High surface areas would be created by the $ZnGa_2O_4$ appearance for the highly divided Ga-doped ZnO powder in comparison with the solid state route. Indeed, from an energetic point of view, the surface always consists in an energy excess: it is well-known that the smaller the powder grain size, the higher the solubility limit of whatever is the substitution ion. The opposite evolution of *a* and *c* cell parameters, that is, the anisotropic cell expansion while gallium concentration inside zincite increases, can be explained based on the bond valence (as defined by Brown et al.[18]). Actually, the *c*/*a* ratio decreases versus gallium concentration

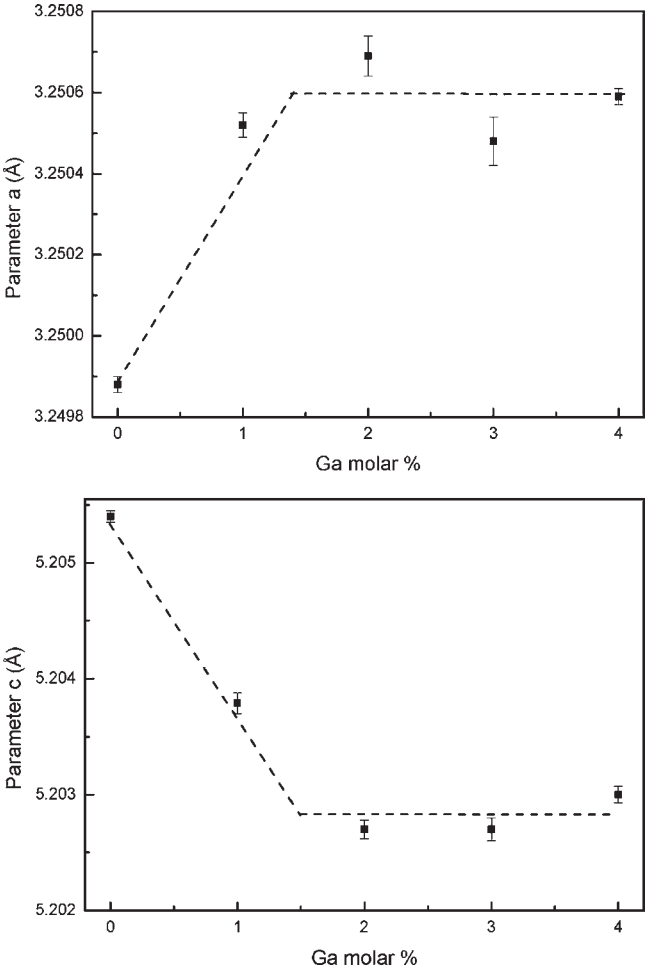

Figure 3. Evolution of the *a* and *c* cell parameters versus the target gallium rate of $Zn_{1-x}Ga_xO$ powder obtained by the Pechini process.

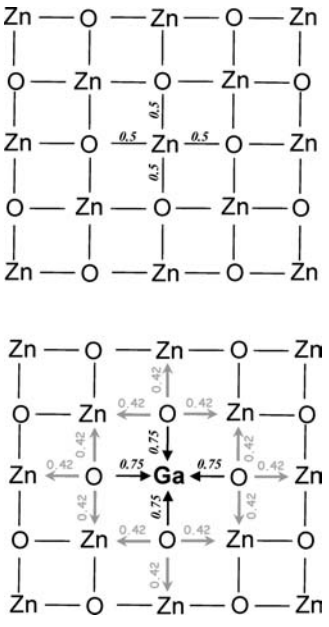

Figure 4. Bond valence representation for a pure and a doped zincite.

showing that the average tetrahedral sites become more isotropic. A representation of the bond valence inside zincite is reported on the Figure 4-top. All the valence bonds in ZnO

(18) Brown, I. D.; Altermatt, D. *Acta Crystallogr., Sect. B: Struct. Sci.* **1985**, *B41*, 244–247.

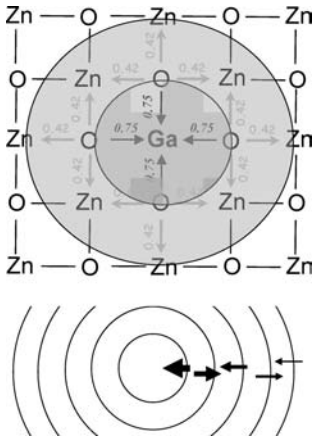

Figure 5. Illustration of the gradual domino effect (expansion/contraction/expansion) through the crystal from a substituted Ga^{3+} ion.

are, in first approximation, equal to 0.5, the oxidation degree of oxygen being −II, that of of zinc being +II, and both elements (cation and anion) are in tetrahedral coordination. The Figure 4-bottom allows a comparison with the previous representation. The modification is the introduction of Ga^{3+} ion. In this model, one free electron, necessary for electroneutrality conservation, is considered completely delocalized, and because of a very low substitution rate, its effect on the valence bond is neglected. Hence, around the gallium ion, the bond valences are forced to be 0.75 to respect the oxidation degree of gallium ion. These Ga−O bonds in a 4-coordinated site are shorter than the Zn−O of the matrix taking as reference either the Brown and Altermatt[18] or the Shannon and Prewitt[19] database. The situation of the oxygen ions linked to the Ga^{3+} becomes unstable, and to respect the −II oxidation degree of these ligands, the sphere of all the O−Zn bonds in second-neighboring position besides Ga^{3+} have to be elongated to reach a bond valence of 1.25/3 (0.42). Then, by a gradual domino effect as illustrated in Figure 5, the propagation of an soften contraction−expansion phenomenon through the whole crystal occurs. The tetrahedral sites of the ZnO matrix (the building blocs) are anisotropic, literature data reporting Zn−O bond about 1.97 Å along the *z* axis, the 3 other ones equal to 1.92 Å.[20−22] The macroscopic expansion of the *a* parameter and the macroscopic contraction of the *c* parameter may be issued from the substitution of Zn^{2+} by a more "isotropic" cation as Ga^{3+} (decreases of the *c*/*a* ratio). Indeed, it was previously discussed in one of our previous publications dealing with ZnO:Co, which is a solid solution constituting a strong analogy since the Co^{2+} ions are inserted in more isotropic tetrahedral sites than the ZnO matrix tetrahedral ones, the structural relaxation of the constraints subsequent to the Zn^{2+} substitution by Co^{2+} ions. A shift of the triangular face of the doped tetrahedral sites toward the *c* axis leading to an anisotropic cell deformation was already proposed herein.[23]

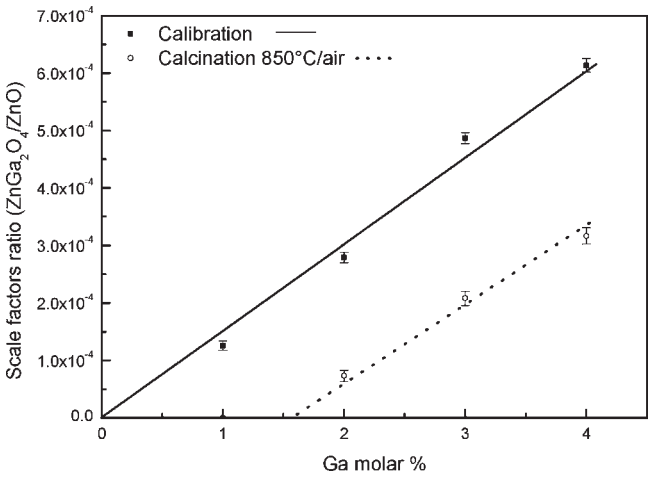

Figure 6. Powder XRD on the $Zn_{1-x}Ga_xO$ samples prepared at 850 °C by the Pechini process.

It can been recalled that carrier-concentration direct measurements from the determination of the electrical resistance, used on the 1500 °C powder set, are not possible on the 850 °C powder set since for such measurements a high temperature annealing is required to obtain ceramic pellets with a negligible effect of the grain boundaries on the total resistance; ceramic sintering is here prohibited since the solubility limit would be drastically reduced during the annealing step.

The solubility limit of the Ga^{3+} incorporated into the ZnO matrix can be more accurately assessed from Rietveld refinements. All the diffraction patterns exhibit zincite as main phase and, for the Ga-rich compositions, $ZnGa_2O_4$ as secondary phase. The amount of the crystallized phases in the sample can be obtained from the final value of the refined scale factor for each phase. A calibration curve was preliminarily established from $ZnGa_2O_4$/ZnO mixtures, prepared by mixing mechanically these two pure phases, annealed at 850 °C under air, with various known ratios. No chemical reaction occurred. The plot of the $ZnGa_2O_4$/ZnO ratio of the refined scale factors obtained from these mixtures versus the Ga content is a linear function with 0 as origin as it can be seen in Figure 6. The plot of the same scale factors ratio refined in the case of as-prepared Ga-doped ZnO samples versus the gallium molar percent is a linear curve parallel to the calibration curve. The parallelism of these two lines indicates that all the matter is in crystalline form, that is, no amorphous phases are present. The later plot enables to assess the content of gallium actually incorporated in the ZnO matrix. Indeed, this solubility limit corresponds to the interaction of the linear function with the *x* axis. After a thermal treatment at 850 °C under air, the Pechini process leads to incorporate about 1.5 mol % of gallium in the ZnO matrix, a value which can be correlated to the one deduced from the evolution of the *a* and *c* cell parameters.

Finally, a last technique has allowed determining the solubility limit in ZnO: the inductive coupled plasma spectroscopy (ICP) titration. The spinel-type $ZnGa_2O_4$ phases are insoluble in chloride acid solutions (20 wt %). On the contrary the zincite-type phases are soluble. Hence, it was easy to only dissolve the zincite-type phase and to perform Ga^{3+}/Zn^{2+} chemical titration in the $Zn_{1-x}Ga_xO$ oxide. The results obtained by the ICP titration are reported in Figure 7. The solubility limit can be deduced and corresponds to about 1.7 mol % of Ga with this last technique.

(19) Shannon, R. D.; Prewitt, C. T. *Acta Crystallogr., Sect. B: Struct. Sci.* **2006**, *48*, 686–692.
(20) Kim Young-Il, K.; Page, R. *Appl. Phys. Lett.* **2007**, *90*, 101904−1–101904−3.
(21) Yamashita, A.; Hansson, R.; Hayes, P.C. *J. Mater. Sci.* **2006**, *41*, 5559–5568.
(22) Yoshio, K.; Onodera, A.; Satoh, H.; Sakagami, N.; Yamashita, H. *Ferroelectrics* **2001**, *264*, 133–138.
(23) Gaudon, M.; Toulemonde, O.; Demourgues, A. *Inorg. Chem.* **2007**, *46*(26), 10996–11002.

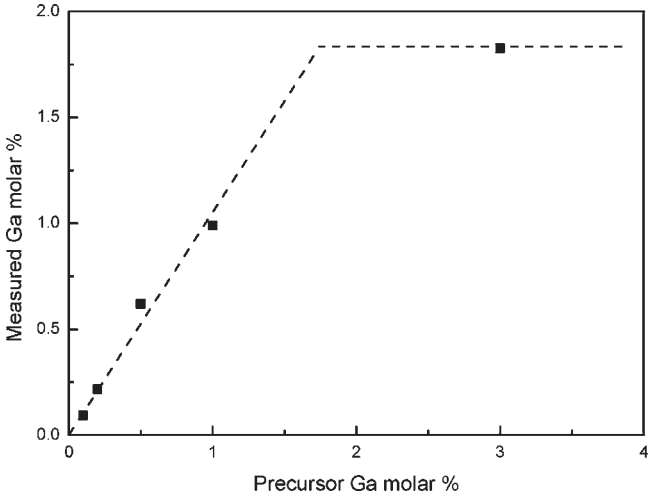

Figure 7. ICP Titration on the $Zn_{1-x}Ga_xO$ samples prepared at 850 °C by the Pechini process.

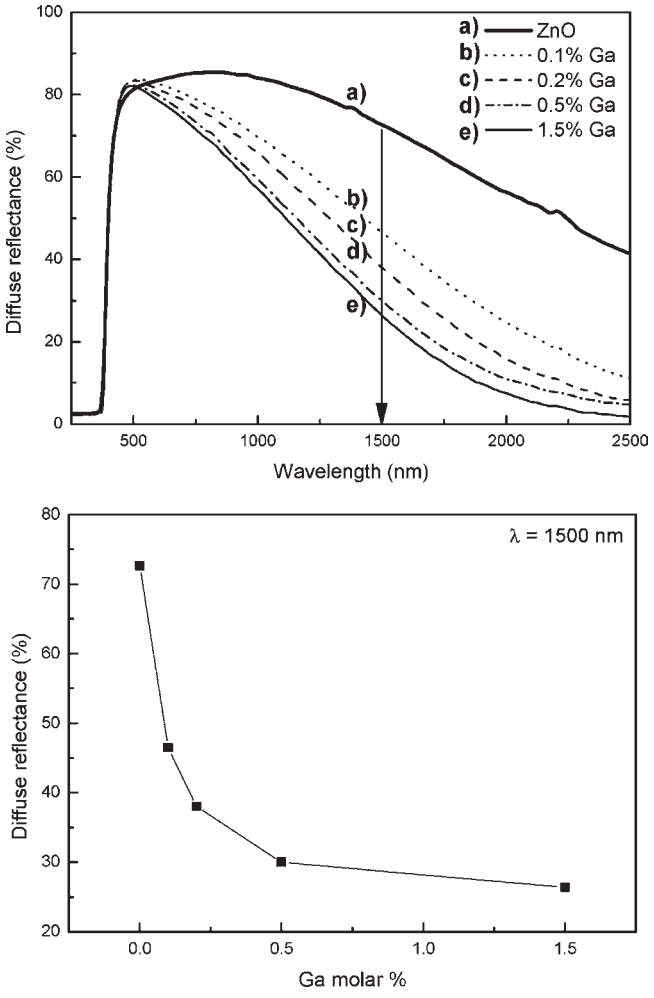

Figure 8. Diffuse reflectance of the (850 °C/under argon) $Zn_{1-x}Ga_xO$ powder for various gallium concentrations.

It was already shown in previous papers[13,14] that the n-type carriers concentration in doped and non-doped ZnO directly depends on the oxygen partial pressure $p(O_2)$ of the synthesis atmosphere. It was demonstrated that a reductive gas is necessary to produce n-type defects concomitant to the substitution by an aliovalent M^{3+} ion. The optical properties

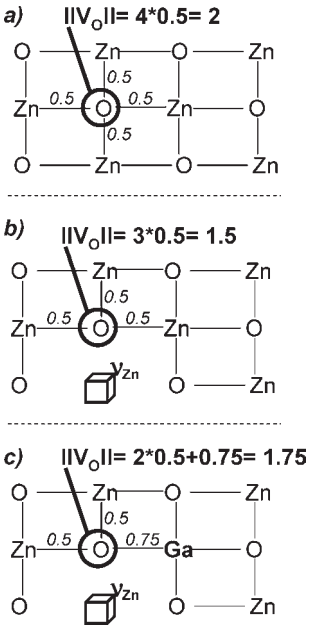

Figure 9. Representation of the stability of pair defects v_{Zn}''/Ga^{3+} (c) in comparison with a single vacancy v_{Zn}'' defect (b).

of the TCOs being directly dependent on the carrier concentration, the effect of the post-annealing under argon of the Ga^{3+} doped ZnO powders was here indirectly evaluated from diffuse reflectance spectroscopy. The optical properties of the various $Zn_{1-x}Ga_xO$ compositions post-annealed under argon are reported in Figure 8-top. The impact of the gallium substitution on the infrared properties is clear: higher the substituting concentration, higher the IR absorption. This observation clearly shows the efficiency of the substitution besides n-type carrier concentration. Nevertheless, the reflectivity intensity versus the $x(Ga^{3+})$ concentration decreases not linearly but follows an asymptotic decrease law. This saturation phenomenon is brought to the fore in the Figure 8-bottom where the reflectance of the oxides at the wavelength of 1500 nm is reported. One explanation which could be proposed is the stability of a cationic vacancy associated with one Ga^{3+} ion taking into account the energy excess induced by only a single cationic vacancy. Actually, cationic vacancies are p-type defects acting to the detriment of the IR absorption induced by n-type carriers, that is, p-type vacancies act as "electron killers" by a mechanism of defect recombination. For illustration, the bond valences around one single cation vacancy and one pair defect are compared in Figure 9. Then, it can be shown that the total valence of an oxygen anion with one vacancy and one Ga^{3+} in their vicinity is less "destabilized" (Figure 9c) than an oxygen anion linked to a single vacancy (Figure 9b). It hence can be considered that more gallium is introduced, and more cationic vacancies can be created; the superposition of these two phenomena leads finally to a maximal rate of n-type defects which can be created by aliovalent substitution in the zincite matrix.

IV. Conclusion

A soft chemical process based on polymeric sols (Pechini route) allows substituting up to 1.5 mol % Ga^{3+} for Zn^{2+} ions into the ZnO framework whereas most previous works were unclear about the maximum rate of aliovalent cations that can be stabilized. XRD analyses coupled with chemical

titration (ICP) and electrical conductivity allow the accurate determination of the solubility limits of gallium inside ZnO depending on synthesis history. From a structural point of view, the doped-ZnO c/a ratio decreases significantly with the Ga^{3+} content. The ionic radii of Ga^{3+}, closer to the Zn^{2+} than the Al^{3+} radii, allows a higher substitution concentration in the case of Ga^{3+} ions, and thus, leads to enhanced electrical conductivity and IR barrier properties. The zincite anisotropic distortion created by Ga^{3+} insertion was explained from the bond valence behaviors. The optical properties of the Ga-doped ZnO show an increase of the IR absorption linked to the gallium concentration introduced. Moreover, the characterization of the optical properties leads to the conclusion that the Ga substitution into the zincite structure is followed especially in the case of high Ga^{3+} rate by the creation of cationic vacancies. These p-type defects limit the concentration of charge carriers; then, a saturation regime besides the improvement of the IR absorption occurs.